



Effect of spatial moving structure and topology optimization of the CNC turning machine tools

Tzu-Chi Chan¹ · Sabbella Veera Venkata Satyanarayana Reddy¹ · Aman Ullah² · Bedanta Roy¹

Received: 27 July 2023 / Accepted: 9 October 2023 / Published online: 20 October 2023
© The Author(s), under exclusive licence to Springer-Verlag London Ltd., part of Springer Nature 2023

Abstract

In order to enhance the accuracy and productivity of CNC machine tools, the finite element method (FEM) is utilized for analyzing machining operations and machine tool structures. Through this approach, it becomes possible to assess and reduce machining errors, thereby improving the precision of machined parts. Additionally, by subjecting machine tool components to the analysis of stress and deformations under real operating conditions, the overall performance and lifespan of the machine tool structures can be augmented. This study focuses on the implementation of finite element methods for the analysis and optimization of CNC machine tool operations and structure. In this study, a virtual model of the Good Way CNC turning machine was used to study the machine's behavior. The first three vibrational modes analyzed through a modal analysis were 108.2 Hz, 133.4 Hz, and 191.7 Hz, which were experimentally validated using modal tests. The design precision was supported by the harmonic response. For an applied external load of 500 N on the head chuck, the tool turret's transient response was established through transient analysis at 0.4 s. However, after the static analysis, the maximum deformation of the machine at the same external applied load on the tool turret was upheld at 7.6 μm . The spatial position analysis rectified the modal performance of the machine at a variety of set working positions. As the principal cause of rigidity originates from the base of the machine, three sets of ground support combinations were claimed to test the machine's rigidity. After the topology optimization analysis was achieved, a better-optimized version of the design was suggested. The old and new models were compared, and an increase of 1.5% in the first three modal frequencies was observed.

Keywords Rigidity · Structural optimization · Static and dynamic performance · Precision engineering

Abbreviations

m	mass of the system (kg)
k	stiffness coefficient (N/m)
c	damping coefficient (Ns/m)
ω	angular frequency (rad/s)
$f(t)$	applied force as a function of time (N)
$u(t)$	displacement as a function of time (m)
$x(f)$	frequency domain representation of displacement (m/Hz)
Φ	mode shape vector

1 Introduction

The design of the CNC machine determines its precision and accuracy. When working with very small tolerances, various physical factors, such as vibrations, the static stiffness provided by the machine, the reaction force at the time of impact with the workpiece, tool deflection, etc., can significantly impact the final quality of machining. To estimate the range or period of disturbances caused by such factors, the main focus of this research is to find the elements involved in causing such disturbances and provide an optimal solution by improving the design. Experimental modal analysis, operational modal analysis, and numerical model analysis are the three types of modal analysis available. Impact tests and an excited mechanical structure using a hammer or shaker are the foundations of experimental modal analysis techniques. The frequency response functions are calculated, and the modes and modal damping are estimated. Numerical model analysis was made using the ANSYS FEA software package. The finite element approach can be useful to determine

✉ Aman Ullah
D1175105@nfu.edu.tw

¹ Department of Mechanical and Computer-Aided Engineering, National Formosa University, Huwei Township, Yunlin County 632, Taiwan, Republic of China

² Department of Power Mechanical Engineering, National Formosa University, Huwei Township, Yunlin County 632, Taiwan, Republic of China

which physical attributes of a machine are required and which can be ignored. FEA could be a powerful tool to utilize for its time-saving ability and economic benefits [1]. Commercial CAE software for use in manufacturing engineering education was offered by Doyle et al. [2]. Zaeh et al. [3] utilized the finite element technique (FEM) to simulate and predict the massive deformation behavior of machine tools. Mackerle [4] examined the 1976–1996 machining analysis and simulation using FEM.

The dynamic properties of machine tool structures are highly correlated with the operating speed [5]. Besharati et al. [6] investigated a gantry-type machine tool using FEA for structural optimization and cost-cutting procedures. They experimentally validated the design using impact hammer modal tests and a genetic decision-making algorithm. Tunc et al. [7] found that the effect of a lower-order frequency is hardly experienced by a milling machine even at lower cutting depths, as the machine governs stability, resulting in a completely different behavior. To verify the influence of natural frequencies and structural characteristics on the processing quality, Chan et al. [8, 9] implemented FEA to extract the static and dynamic features of the machine. An AIM polynomial was used to establish a prediction model for the quality processing of a five-axis machine. Several modal analysis techniques are widely used to investigate a structure's dynamic properties by identifying the modal parameters. Mbarek et al. [10] proposed a comparison of an experimental modal analysis (EMA) test, an operational modal analysis (OMA) test, and an order-based modal analysis (OBMA) test performed on a planetary gear for recirculating energy. Yang et al. [11] suggested a method that is a general kinematic modeling technique with primary use in the study of motion and machining accuracy analysis of multi-axis CNC machine tools. The kinematics equation form is the same whether one is modeling the motion of a multi-axis CNC machine tool using the motion shaft model or the POE model of the motion system. Wang et al. [12] used the Taguchi experimental design approach to produce the components with varying specifications by orthogonalization of the dimensional parameters, and an IDM of dimensional parameters and structural topology is proposed based on the improved stiffness-mass metamodeling to fill the gaps in the model. Chauhan et al. [13] proposed the dynamic description of a wind turbine transmission. They used a finite element model to identify its mode shapes and compared the numerical mode shapes to those acquired experimentally. Experimental modal analysis and transient analysis in the ANSYS workbench were utilized to verify the precision of a moving column grinding machine. Chen et al. [14] and Wu et al. [15] evaluated the same dynamic and static parameters for a hydrostatic spindle and a machine tool, respectively. Harmonic response analysis was implemented in the ANSYS workbench to evaluate the design

response to an externally excited frequency. The acquired results are sufficient to prove the modal frequency of the machine obtained by modal analysis and the probability of resonance while working. Lu et al. [16] verified a gantry machine tool crossbeam using FEA and concluded the effect of frequency on the rigid behavior of the machine. A high-speed five-axis machine tool was tested for its internal frequencies, stiffness in static conditions, and variable position, and was evaluated for its transient response. Based on the results, the bed was redesigned to improve the results further [17].

It is preferable to reduce the majority of the weight of the CNC machine while maintaining sufficient stress to withstand external loads during the research process. Hong et al. [18] used CAE with commercial software as a research method to analyze the linear static construction, stress, and deformation for the secondary shaft system, primary shaft system, and machinery bed in a large five-axis turning-milling complex CNC machine. Chan et al. [19] used topology optimization to create effective structural optimization designs. The best topology optimization conditions included lightweight structures, which resulted in less structural deformation and higher natural frequency. Huo et al. [20] used simulation modeling to evaluate the analytical features and thereby used an integrated design. The machine was tested for both open- and closed-frame configurations using ANSYS, and the results provide scope for design optimization. Li et al. [21] optimized a crossbeam of a CNC milling machine using the NSGA-II algorithm. The process helped to reduce the deformation by 3.08% and increase the modal frequency by 0.42%, improving the machine's resistance to resonance. Using the orthogonal experimentation method, Deng et al. [22] increased the optimization efficiency. Qiu et al. [23] analyzed the torque-angle characteristics of LAL-CTFH, the four-bar linkage PRBM (FB-PRBM) for LAL-CTFH was proposed as an enhanced pseudo-rigid-body model (PRBM) technique. By using finite element analysis (FEA), the method was validated. The LAL-CTFH's constant-torque output characteristics were also improved. The optimized model is put through theoretical analysis, FEA, physical prototype manufacture, and experimental testing, respectively. The findings demonstrate that the proportion of constant-torque output can increase to more than 65% in the 0–40° range and that the average error between theoretical value and test value is less than 5%. This validates the viability of the design strategy and the accuracy of the theoretical analysis. Further preceding investigation on innovative optimization techniques has been discussed in an orderly fashion.

Using a structural design optimization of surface method (RSM), a new hybrid algorithm that integrates simulated annealing (SA) and particle swarm optimization (PSO) algorithm is developed to solve the structural optimization

problem. The maximum lightweight results in a reduction of energy consumption by 3.22% and moving component mass by 8.14%, whereas it increases the first natural frequency from 298.23 Hz to 306.9 Hz by a factor of 2.91%, and increases maximum deformation and stress values for the part in consideration [24]. Zhong et al. [25] investigated multi-objective optimization and finite element analysis and developed the code for this method. The structural stiffness of the optimized framework increased by 89% compared with the original, despite the 6% increase in mass and 9% increase in material costs. Park et al. [26] established a new approach in Analytical methodologies and experimentally validated this comprehensive strategy. A penalty function for the tiny milling machine was calculated using the mathematical model to identify the ideal structure. The optimal size of the machine tool structure determined by analytical and FEA approaches differed by 10%. Wang et al. [27] used Taguchi's method, the FEM, and Gray relational analysis (GRA). The ideal target structure in his investigation had a maximum dynamic deformation of 486 μm at 35.9 Hz, compared to 148 μm at 40 Hz. Ibrahim et al. [28] utilized discrete derivatives, computational differentiation, overall finite differences, and continuum derivatives. The test findings supported the accuracy of the finite element analysis, with a stress level deviance ranging from 7.75 to 10.24% when compared to the numerical values.

Previous studies' findings not only encourage further lightweight design of CNC machine tool components but also give several helpful references for this paper's investigation. In this paper, we advance the state of the art beyond the single-goal optimization of large datasets and the direct use of existing optimization techniques within ANSYS. This paper aims to implement FE analysis and proceed with modal, static structural, transient, and harmonic response analysis to investigate the dynamic and static characteristics of the GA-3300 horizontal turning slant bed CNC machine. The computer-aided design is validated through a modal test experiment performed using an impact hammer, an accelerometer sensor, and a digital FFT analyzer. The paper also includes spatial position analysis, performed by moving the parts to distant locations and observing the changes in the machine's internal vibrations and static stiffness. Based on the results, the machine bed, being the prominent cause of rigidity and the heaviest of all the parts, is redesigned to further improve the solutions of static and modal analyses. The ground supports provide a reasonable amount of rigidity to the machine, and various combinations are tried to improve the machine's stiffness. The topology optimization module in ANSYS provides an optimal solution without affecting the base configuration's ability to withstand the externally applied loads. As shown in Fig. 1, the basic structure of the turning CNC machine tool is configured with three axes (x -, y -, and z -axis), and the suggested technique

can appropriately describe the static and dynamic properties of machine tools.

2 Methodology

Several books have presented the fundamentals of finite element analysis, including Zienkiewicz et al. [29] and Bathe et al. [30]. White et al. [31] used the intermediate-complex method, which is more efficient than a fully resolved finite element simulation but more general than beam theory or homogenization. Gil et al. [32] present a general method for computing the dynamic response of periodic infinite structures under a moving load. In this study, the CAD model is imported into the ANSYS workbench for FEA characteristics and to validate the aforementioned analysis technique, which is illustrated in Fig. 1. It is examined using FEA and theoretical calculations. where $[k]$, is the element stiffness matrix, $[\delta]$ is the nodal displacement vector of the element, and $[F]$ is the modal force vector. These element qualities can be formulated using one of four methods: the direct technique, the variation method, the weighted residual method, or the energy balance method. After putting together the characteristics of an element using any of these approaches, the variation method is widely used in the field of solid mechanics to construct stiffness matrices and nodal force vectors (constant loads). System equations are constructed using global/structure properties that are assembled using element properties.

$$[K]_e \{\delta\}_e = [F]_e \quad (1)$$

Therefore, the finite element analysis consists of the following stages:

-
- | | |
|---|--|
| <ul style="list-style-type: none"> • Determine which field variables and ingredients will work best. • Condemn the continuum. • Pick out some interpolation routines. • Identify the features of the element. • Put together local attributes of individual elements to get global ones. | <ul style="list-style-type: none"> • Put the boundaries in place, as required by • Get the nodal unknowns by solving the system equations. • Perform the further computations necessary to obtain the specified values. |
|---|--|
-

2.1 Material properties

The machine model is imported into the ANSYS software interface, and the process begins by assigning the materials associated with the parts. Grey cast iron is chosen for most of the parts because of its lower density compared with structural steel and smaller expense. The physical machine also uses the same material for its heavy parts, accounting

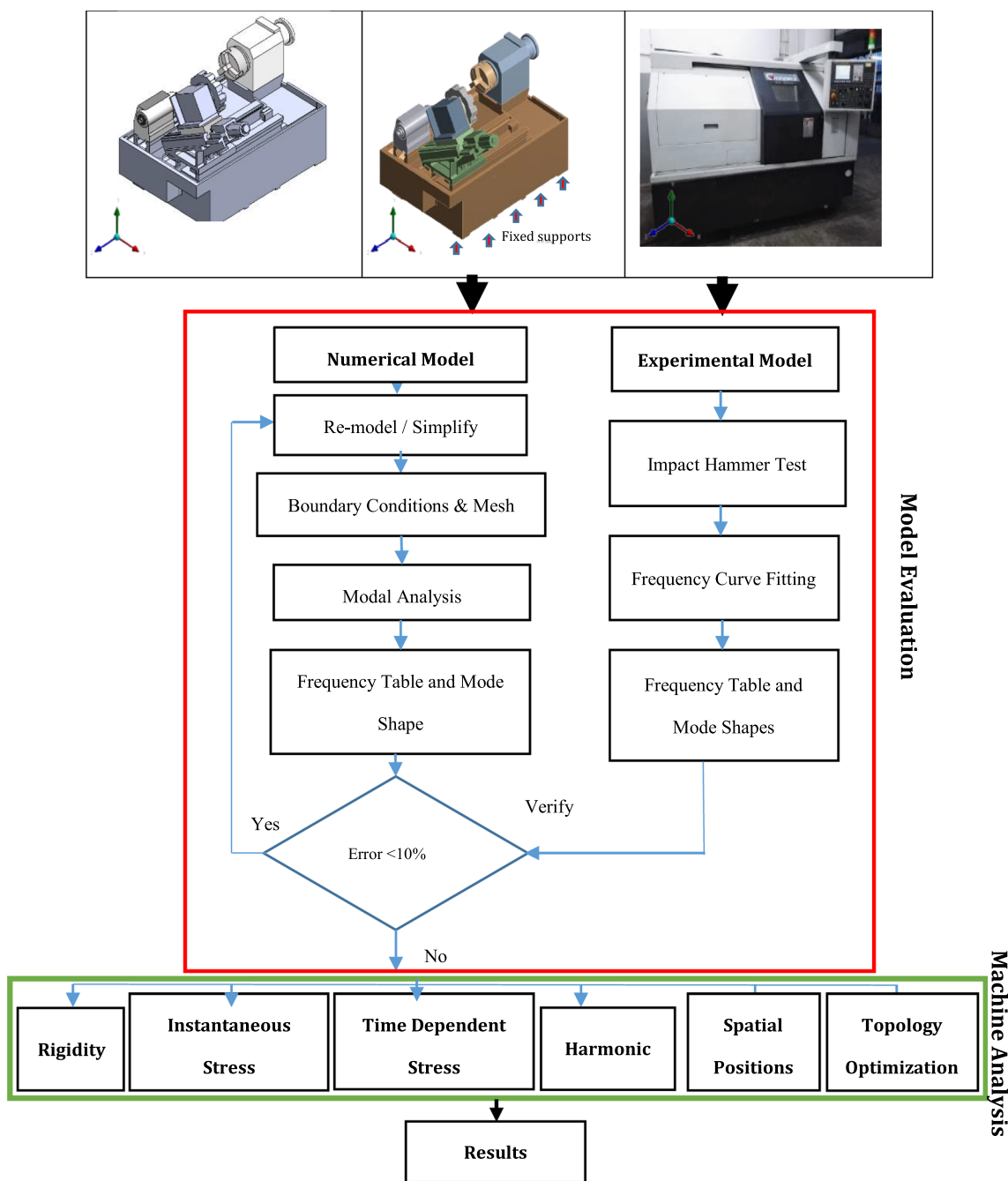


Fig. 1 Framework of the machine model and the working methods

for less structural weight. The tool turret and the head chuck have structural steel (SS) properties, which are listed in Table 1.

2.2 Mesh sensitivity and mesh independence study

The generated CAD models were transferred to the ANSYS Workbench to create finite element models. The first stage step was the meshing procedure. The mesh-generation process is critical to finite element analysis. The calculation’s precision

Table 1 Material properties

Property	Structural steel	Grey cast iron
Density (kg/m ³)	7850	7200
Young’s modulus (Pa)	2*10 ¹¹	1.1*10 ¹¹
Poisson’s ratio	0.3	0.28

is proportional to the size of the mesh utilized. The results can be recognized more if the mesh is smaller, but this comes at a large cost in processing time. To begin, a preliminary mesh

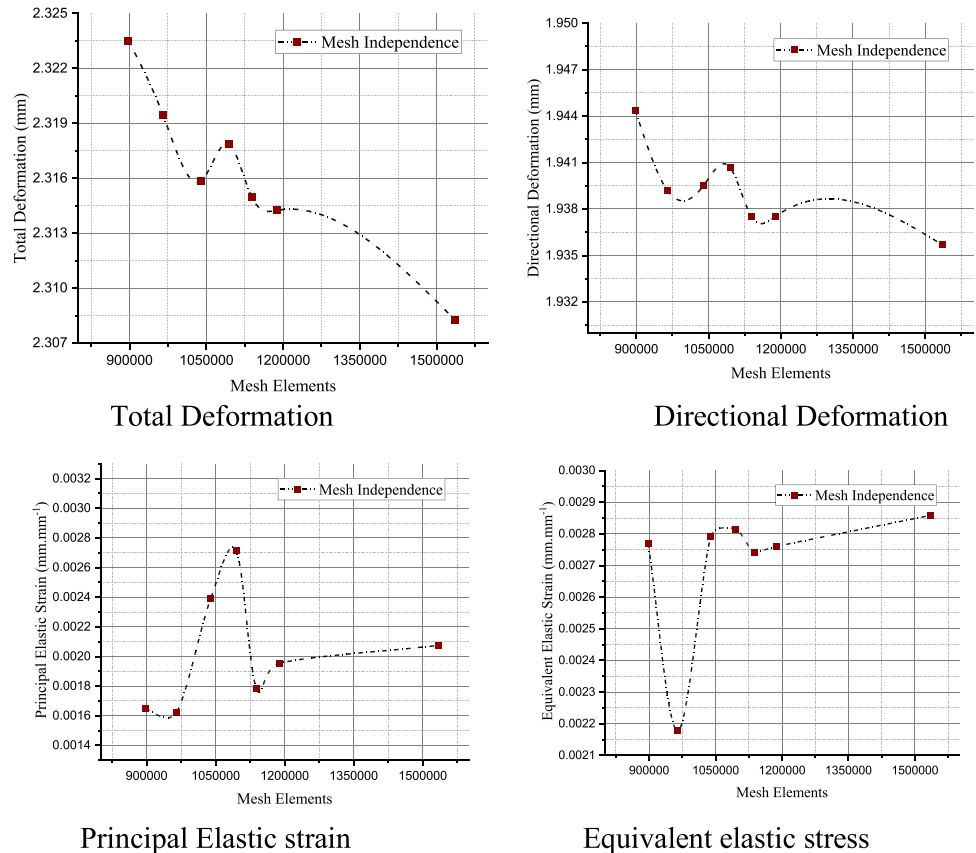
generation is performed to determine the best balance of mesh quality and processing time. The mesh of the model is separated into several components during the analysis. The patch-confirming algorithm in the software is used to produce a finer and more accurate mesh. The tetrahedron method is applied due to the fact that the machine contains multiple solid shapes and curves. An element’s degree of freedom should not be compromised in order for the solution to converge with the experimental results. With a quadratic element order, the grid around the body has the greatest number of nodes and elements. Starting from 70 mm, the element size is brought down by 1 mm each time to find the best fit for the overall analysis. The meshing was successful at an element size of 25 mm. The mesh metrics of the nodes and the number of elements are given in Table 2.

The slider contacts are bonded joints between the parts and rails. The contact region detection setting is changed from the default “program controlled” to “nodal normal to target,” and the normal stiffness factor is changed from the default of “1” to “0.2.” This setting provides a solution that converges with the experimental data with less error.

Table 2 Mesh metrics

Nodes	Elements
1,872,232	1,188,584

Fig. 2 The finite element model’s mesh convergence test results



In order to ensure that the FE analysis was accurate for each situation, mesh convergence tests were conducted. Results from mesh convergence tests were analyzed to see how directional deformation, total deformation, principal elastic strain, and equivalent elastic stress changed throughout a range of element matters. Figure 2 shows how the values of directional deformation, total deformation, principal elastic strain, and equivalent elastic stress changed as the number of mesh elements increased. After the ninth point, however, the deformation variation stabilized. Therefore, a procedure for the element size meshed in finite element analysis (FEA) was established, and the converged mesh number was determined; this allowed the natural frequency to fall within the 1% convergent range in the convergent analysis of the three-dimensional geometrical models of the individual subsystems.

3 Validation

To graphically test the machine, the CAD model should be harmonized with the physical model. Properties such as weight and materials can be assigned, but to tone with the characteristics, at least one analytical measure should match the experimental results within a certain span of

error. In this study, the experimental results of vibration testing are compared with the modal analysis results of computer-aided design. This process validates the resemblance of features, allowing us to proceed with further studies on the machine, sketching, and remodeling if possible. To correctly detect the internal frequencies of a system, it is important that the size and shape of the body represent the physical geometry.

3.1 Modal analysis

A preliminary modal analysis is carried out on the static machine considered to be at rest in order to find the free vibrations of the machine. The modes of vibration depend on the system mass, stiffness, and spatial distribution of parts. For structures, the damping amount is generally neglected if it is below 10% and if it is considered that there is no external loading. The generalized equation of the motion of a body is as follows:

$$[M] \left[\ddot{U} \right] + [C] \left[\dot{U} \right] + [K] [U] = [F] \quad (2)$$

When the damping and external loading are ignored, Eq. (1) changes to

$$[M] \left[\ddot{U} \right] + [K][U] = [0] \quad (3)$$

Along with the parameters of the boundary conditions in Sect. 2, the range of frequencies in the analysis is set to a minimum of 0 Hz and a maximum of 500 Hz, and the first 10 modes of frequency are evaluated. Damping and loading are ignored. The modal shape deformation of each frequency range is illustrated in Fig. 3 and the frequency response along with its mode shape is shown in Table 3. The 10 modes of natural frequency generated in the ANSYS workbench, considering the first three modes in the frequency table for evaluation as the frequency ranges from the fourth mode, directly affect the base of the machine. Such a disturbance due to vibration tends to move the machine completely and damage the workpiece, resulting in machining errors. When machining chatter occurs, it leads to poor surface quality, a higher rate of parts and tools being thrown away, and high economic losses [33].

3.2 Experimental setup

In a previous study, a back-to-back impact hammer examination was utilized by Bias et al. [34]. The external excitation of a structure using an impact hammer is the pre-eminent method for finding natural frequencies in an easy and inexpensive way [35]. To check the convergence of

the results, an impact hammer modal test experiment is performed on the physical machine. To find the mechanical excitation of a structure, an external impulse is provided to the machine using a hammer. The hammer comes with a configurable tip made of rubber and an extender weight. The sensitivity configuration is adjusted as shown in Table 4 (Hammer). An accelerometer sensor with three-axis calibration is used to record the vibration signals at different points. It contains a piezoelectric crystal generating a force that generates a high-impedance electric charge proportional to the applied impulse and acceleration. The sensitivity calibration is given in Table 4 (Accelerometer). Both of these devices are connected to a Signal Conditioning and Data Acquisition (SCADAS) unit, which is connected to the NOVIAN computer program. The SCADAS/Spectrum analyzer comes with four channels of input and a single output signal. The signal contains coherence, an auto spectrum, a time waveform, and a frequency response function (FRF). The FRF holds the machine's response to an excited frequency. An outline of the process and physical modal testing is shown in Fig. 4.

3.3 Data processing

To evaluate the CAD model, the physical model is tested for its excitation frequency by providing an external impulse with a hammer and recording the generated data. FRF is filtered out using the software features and imported to ME'scope software. ME'scope is a post-processing software that can evaluate the natural excitations of a structure and animate the mode shapes, with built-in calculus functions. A shape table is formed for the first three modes of frequencies and compared with the modal frequency generated in ANSYS. The signals are collected from the machine area that is visible and able to be reached by the sensor, as shown in Fig. 5a. A total of 96 points are drawn from all over the machine, with an average of three impulse hits for each data point. The sensor is calibrated with the sensitivity as directed as per the manual provided by the manufacturer. The machine is positioned similarly to the CAD model, and the experiment is carried out. FRF displays the peaks occurring at a certain range of frequency when plotted. ME'scope software is used to perform the curve fitting and modal shape evaluation, as shown in Fig. 5b.

3.4 Result and discussion

To confirm that the CAD model replicates the physical design, the results from the analytical solution and experimental solutions are compared, as shown in Fig. 6a–c. This is an important step in the research study as it certifies the

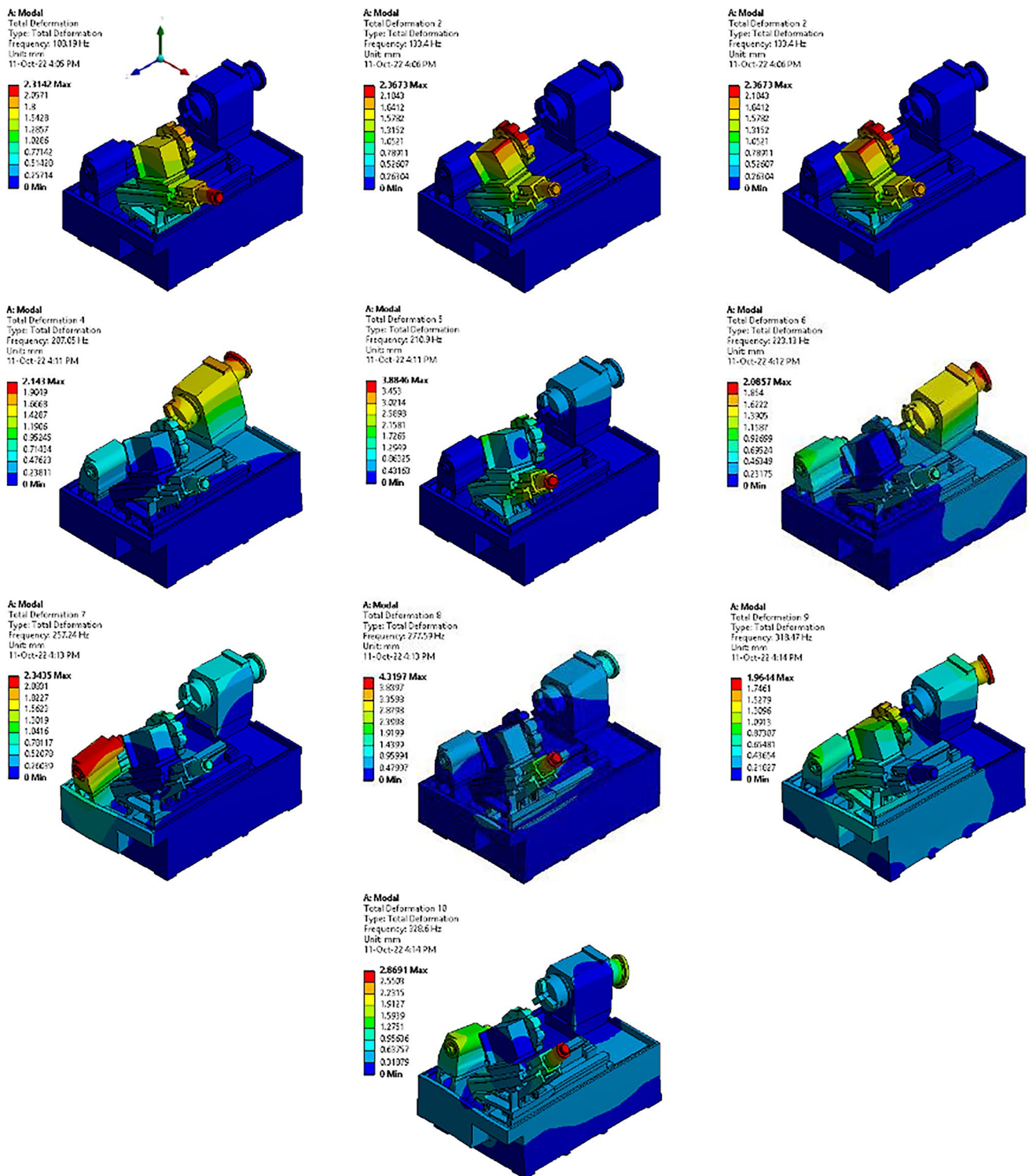


Fig. 3 Deformation at 10 mode shapes

computer sketch and relates all of the parameters set in the analysis. If the results do not agree with each other the model is remade and the simulation settings are changed. If the results match, the set parameters resemble the boundary

conditions of the physical machine, allowing further studies based on computer-aided engineering (CAE). The acquired results of static analysis on the same design can be considered accurate and trustworthy.

Table 3 Modal frequency and mode shapes

Modal frequency table		
Mode	Frequency (Hz)	Mode shape
1	108.2	The axel assembly vibrates along the <i>x</i> -axis.
2	133.4	The axel assembly vibrates along the <i>z</i> -axis.
3	191.7	The tail stock oscillates along the <i>x</i> -axis with small movement on the axel.
4	207.05	The axel twist and the tail stock oscillate along the <i>x</i> -axis.
5	210.9	The head and tail stocks and the axel vibrate along the <i>z</i> -axis.
6	223.13	It has the same movement as the previous mode with a small diagonal motion of the parts.
7	257.24	Along with all the parts the base of the machine has a movement w.r.t parts.
8	277.59	The axel and the headstock twist upward in the <i>y</i> -axis direction.
9	318.47	All 3 parts twist upward disturbing the base.
10	328.6	Twisting motion in all the parts in the direction of the <i>y</i> -axis.

Table 4 Sensitivity configuration

Hammer		
Configuration	Tip	Grey-9912
Sensitivity at 100 Hz	mV/N	0.193
Sensitivity ratio at 100 Hz	N/g	53.69
Accelerometer		
Sensor axis	Sensitivity	
<i>x</i>	103.9 mV/g	
<i>y</i>	104.0 mV/g	
<i>z</i>	104.6 mV/g	

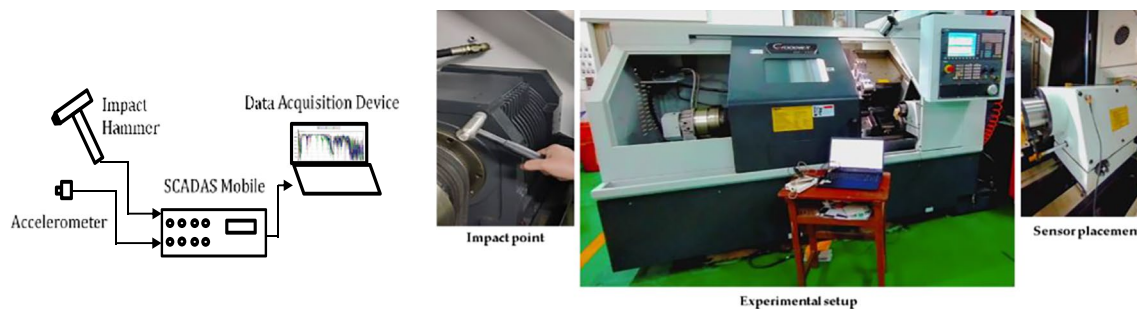
As shown in Table 5 and Fig. 7, the first three modal shape results from the FEA and experiments have an error of 0.7%, 1.2%, and 0.2%, respectively. Having an error of less than 10% verifies that the parameters set for analysis are in accordance with the real condition. The model is confirmed to relate to the physical machine, allowing the research to proceed to the analytical study of the machine, where the machine is tested for its static characteristics.

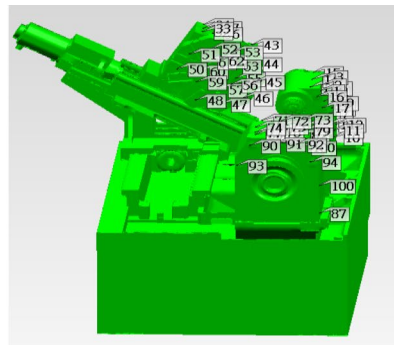
4 Analytical study

Hong et al. [18] carried out static structural analysis on a turning milling complex CNC machine to verify the uniqueness of the design and suggested an optimal possibility to reduce the weight of the machine to further improve its machining process. This paper adapts a similar approach to evaluate the design characteristics using FEA. The effect of steady-state loading conditions under the influence of standard gravity without a time constraint is evaluated in static structural analysis carried out on the machine to find the displacement of the parts, and the static rigidity of the machine is evaluated. The machine is tested for its behavior when an external force of 500 N is applied to the tool. The machine's response to time-dependent loads is evaluated using transient structural analysis. To study the vibrational excitations under the applied load, the harmonic response of the tool turret is observed, as the machining involves the effect of force on the tool.

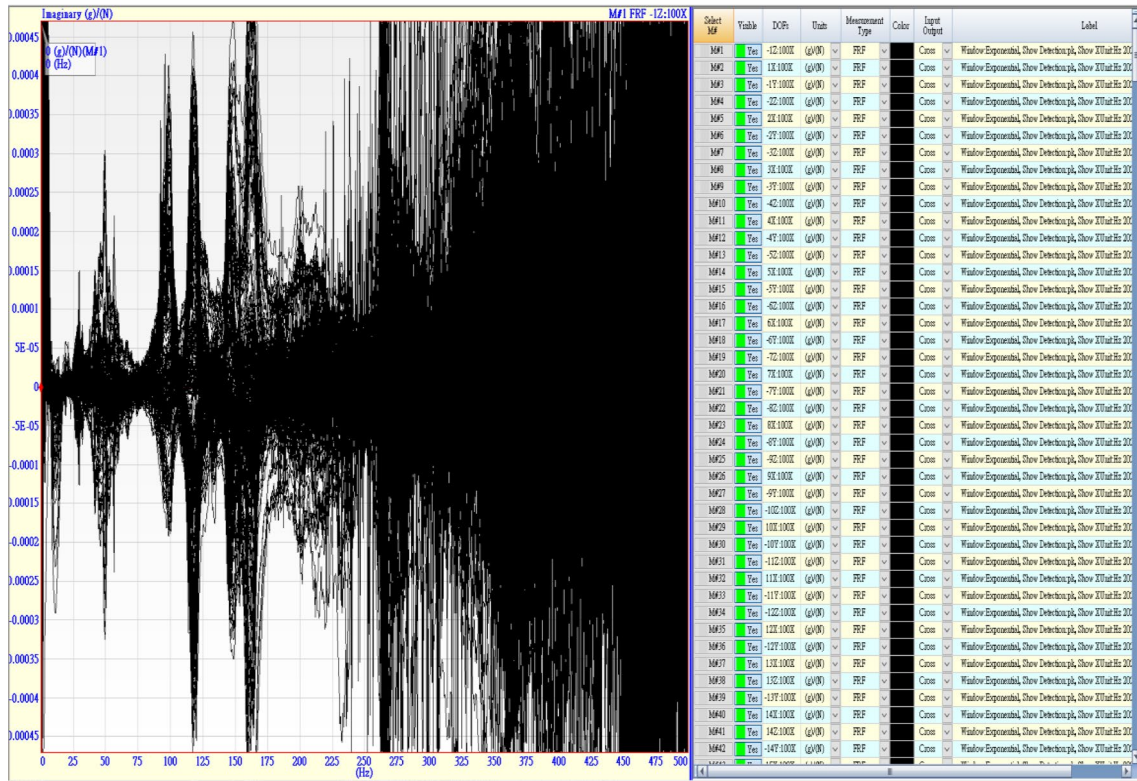
4.1 Harmonic analysis

Similar to the modal testing procedure, the machine is excited and its response recorded, and such excitation

**Fig. 4** Experimental setup



(a) Sensor points



(b) curve fitting and peak identification

Fig. 5 Model analysis ME’scope

is carried out by applying an amount of force using the ANSYS workbench. The point of impact of the force is similar to the experimental testing point, considering that the point sufficiently excites the machine. The part is the same as that used in modal analysis because the excitation range is used to form the results of modal analysis. The range of operation is from 100 to 350 Hz, taken from the modal analysis results. The frequency response of the tool turret is measured. A total of 250 solution intervals are plotted, representing a unit hertz of frequency. The machine responds at a certain frequency, observed through a change in phase angle, as shown in Fig. 8.

Clear peaks around 100 Hz, 150 Hz, and 200 Hz represent the excitation of the machine at a certain frequency, which is similar to the frequency results generated in the modal analysis. The results verify the modal analysis and the accuracy of the results obtained.

4.2 Structural analysis

The solid body analysis deals with the equilibrium of the system in global coordinates. The method of finite element analysis solves for the displacement, induced stresses, and strains due to applied loads using the ANSYS software. The static

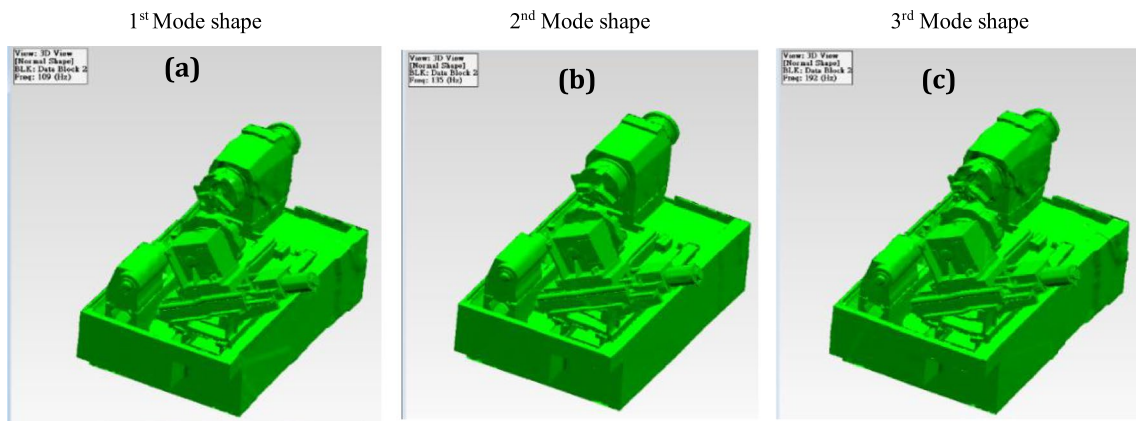


Fig. 6 Modal analysis; a–c modal test—ME’scope

Table 5 Test comparison and error

Impact hammer test and ANSYS result comparison			
Mode	Workbench (Hz)	Me’scope (Hz)	Error (%)
1	108.2	109	0.7
2	133.4	135	1.2
3	191.7	192	0.2

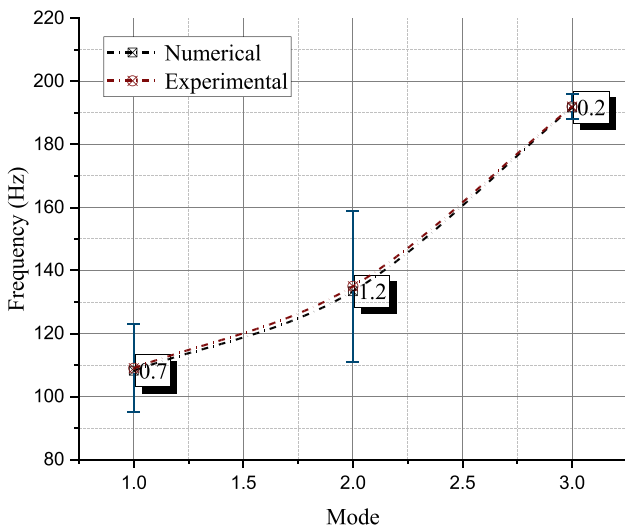


Fig. 7 Comparison between the FE results and the experimental results

analysis ignores the factors of damping and time-variant loads. The governing equations can be given as follows:

$$\frac{\partial \sigma_x}{\partial x} + \frac{\partial \tau_{xy}}{\partial y} + \frac{\partial \tau_{xz}}{\partial z} = 0 \tag{4}$$

$$\frac{\partial \tau_{xy}}{\partial x} + \frac{\partial \sigma_y}{\partial y} + \frac{\partial \tau_{yz}}{\partial z} = 0 \tag{5}$$

$$\frac{\partial \tau_{xz}}{\partial x} + \frac{\partial \tau_{yz}}{\partial y} + \frac{\partial \sigma_z}{\partial z} = 0 \tag{6}$$

Where σ_x , σ_y , and σ_z are the normal stress components and τ_{xz} and τ_{yz} are the shearing stress components. For the finite element method, the same computations are carried out in the matrix form;

$$[K]\{\delta\} = \{F\} \tag{7}$$

where $[K]$ is the element stiffness matrix, $\{\delta\}$ contains the nodal displacement vectors of elements u , v , and w regarding the global coordinates in the x -, y -, and z -axes, and $\{F\}$ represents the nodal forces element vector in the x -, y -, and z -axes. The total displacement (deformation) due to the applied load on the tool turret is $7.6 \mu\text{m}$, as shown in Fig. 9. The maximum occurs on the tool turret and the minimum on the base of the machine.

4.3 Transient analysis

A restoring force is developed to optimize the externally occurring force in a body. This phenomenon is also seen in vibration, as the body tends to rest after a certain amount of time. For a machine of a given weight and dimensions, the program is set to observe for a second. Since the applied force and the obtained result cannot be in the same time slot, a four-step procedure is set. The time slot of 1 s is divided into 0.02 s elements. A force of 500 N is applied to the machine in the first slot, and the number of seconds the machine requires to adjust to the force is observed. Step 2 takes place at 0.04 s, step 3 at 0.5 s, and the fourth step ends at 1 s. Besides the setting of the time steps, all other boundary conditions are identical. The time taken to converge to

Fig. 8 Harmonic response

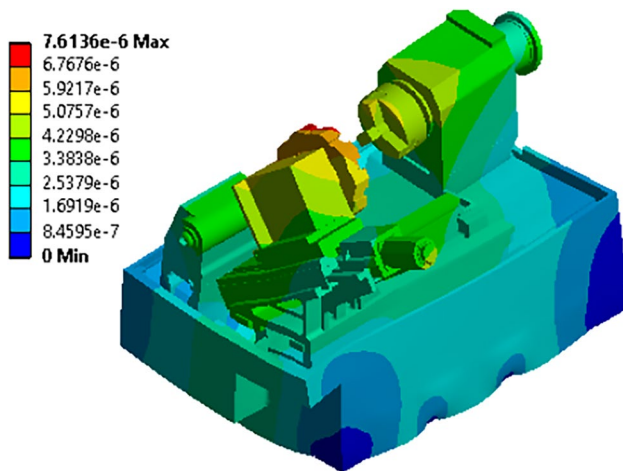
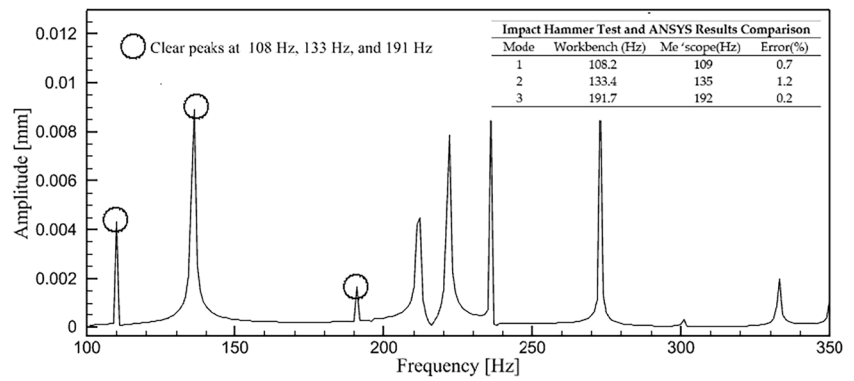


Fig. 9 Total deformation, according to static structural analysis

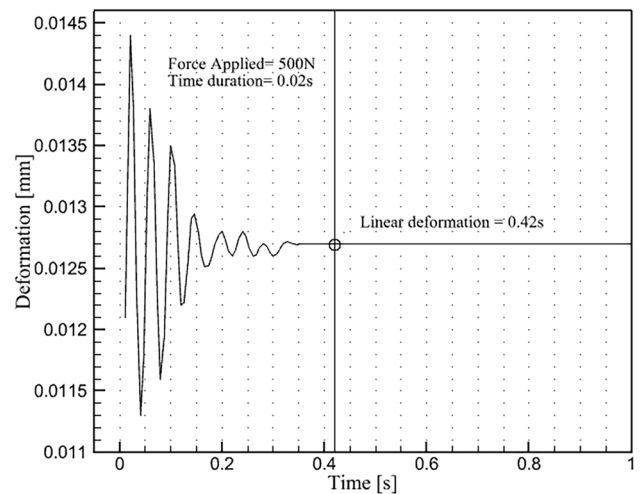


Fig. 10 Transient response

a linear deformation is 0.42 s, which falls within the range of many such machines. The curve is portrayed in Fig. 10.

4.4 Spatial analysis

The performance of the machine changes with respect to the position of the parts. To check the variations caused due to the motion of the parts, the mobile parts are moved to different positions along the guideway and tested for changes in internal frequencies and static rigidity. This procedure is referred to as spatial analysis, as shown in Fig. 11, demonstrating the changes occurring within the machine. There are three moving parts whose position can be altered depending on the physical condition: the axel (A), the tailstock (B), and the tool turret (C). These parts are varied based on the work piece and the operation. The model has a total of 27 spatial positions to which the machine parts can be moved, providing a graphical representation of the behavior of the machine at its natural frequency. The conditions applied are at the initial point (A1, B1, and C1), a middling point (A2, B2, and C2), and the extreme endpoint the parts can reach (A3, B3, and C3). The points taken are the edge-to-edge

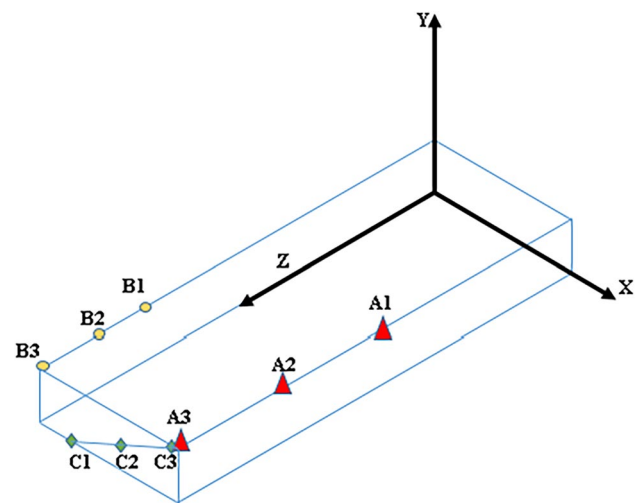


Fig. 11 Spatial positioning plane

distance rather than the midpoint of the part. The machine has no y-axis motion.

All possible combinations of the positions are applied and analyzed for their vibrational and static structural stability. The parts are moved from their initial position (starting/working point) to their extreme end position (resting/no work point). The placement of the parts is given below in Table 6.

From (A1, B1, and C1) to (A3, B3, and C3), the thread lines drawn on the plot represent a decrease in the internal frequency. For the first nine models, where the parts are close to each other as if in a working position placement, the machine has higher range of vibration, which is healthy for a machine to avoid resonance. This also indicates that the concentration of the mass of the parts has a noticeable effect on the dynamic properties of a complex mechanical design. The machine’s internal frequency changes for mode 1, 2, and 3 are shown in Fig. 12.

Table 6 Spatial position-part placement

Part-placement			
Model	Axel (mm)	Tailstock (mm)	Tool turret (mm)
	[A]	[B]	[C]
1	230[A1]	150[B1]	104[C1]
2	230	150	204[C2]
3	230	150	304[C3]
4	530[A2]	150	104
5	530	150	204
6	530	150	304
7	730[A3]	150	104
8	730	150	204
9	730	150	304
10	230	350[B2]	104
11	230	350	204
12	230	350	304
13	530	350	104
14	530	350	204
15	530	350	304
16	730	350	104
17	730	350	204
18	730	350	304
19	230	500[B3]	104
20	230	500	204
21	230	500	304
22	530	500	104
23	530	500	204
24	530	500	304
25	730	500	104
26	730	500	204
27	730	500	304

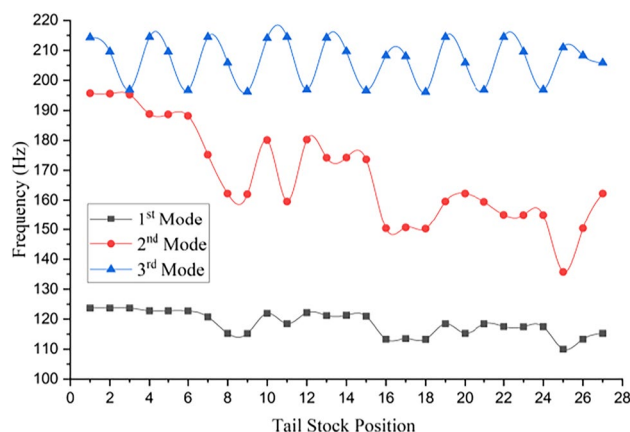


Fig. 12 Machine’s internal frequency changes for modes 1, 2, and 3

From the above study, the properties of the machine under loading and spatial displacement are clearly understood, and this clearly implies that the machine design is sustainable under almost all machining conditions. Since the CAD model also resembles the physical one, slight improvements can be made in terms of increasing the rigidity with a weight-reducing principle and cutting the costs of manufacturing. To improve the rigidity, two methods were considered, which are discussed below. The biggest and heaviest part of the machine is the base. All of the parts rest on the base, and stability is achieved, with structural benefits provided by the bed of the CNC. This research mainly focuses on changing or improving the bed design. Ground support is the key factor in providing a rigid platform.

4.5 Rigidity analysis

To increase the static rigidity of the machine, the type of ground support upon which the machine is rested is changed. The change in the range of frequencies is found by performing a modal analysis on each of the models. Structural analysis is performed to evaluate the machine’s rigidity.

4.5.1 Modal analysis—changed base supports

The machine is evaluated for its virtual design, and moving forward, the machine is tested for its behavior when the type of ground support is changed. Three conditions are considered: First, when the whole machine is placed on the ground, the amount of surface coming into contact with the ground increases, as shown in Fig. 13, which reflects the increasing static rigidity of the machine. In the second condition, the machine has eight ground supports in the physical form, as shown in Fig. 14. The third condition increases the number of supports to 10, evenly spread across the surface area of

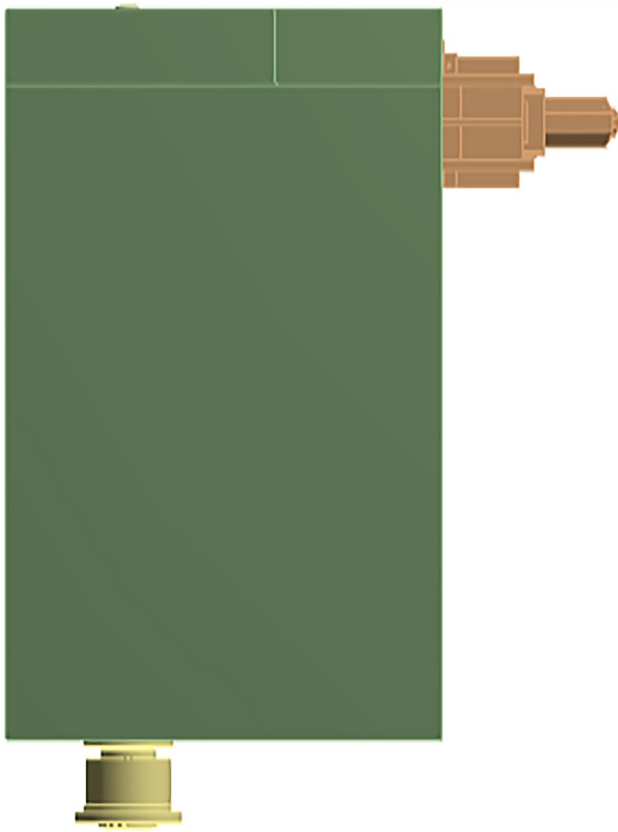


Fig. 13 Model (1)—without ground supports

the base, as shown in Fig. 15. Although the first condition is not possible, it is tested in order to compare the results. The three sets of ground supports are shown below, and their frequencies are given in Tables 7, 8, and 9.

When the ground supports are removed, the machine lies completely on the ground. In this condition, a large amount of surface area is in contact with the ground. The internal frequencies are shown in Table 7. The actual model has unevenly spread supports, balancing the major parts of the machine. When the fixation method is changed, according to the results of model (1), the machine is more rigid compared with the real model. For a design with evenly spread fixation supports, there is a nominal increase in the internal frequencies. A comparative graph of the three tables shows that the distinctive vibrations developed due to changes, as shown in Fig. 16. The noticeable change among the 10 modes of frequency suggests the effect of fixation on the rigid behavior of the machine, as shown in Fig. 16. As predicted, a machining center is fixed to the ground in order to keep up with the vibrations, displacements, and fluctuations during the process. An increase in the surface area of the fixtures makes them stable enough to withstand the chatter. The same principle is applied and the number of ground

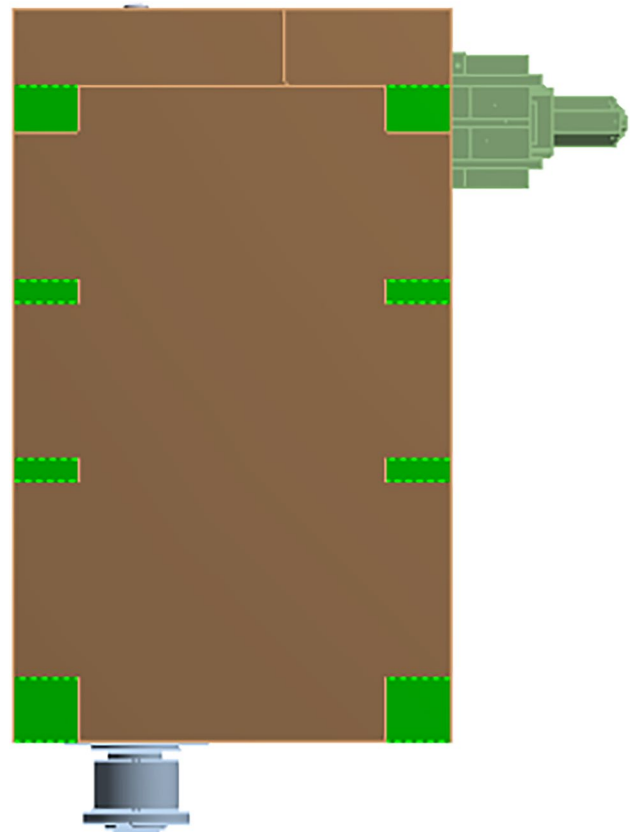


Fig. 14 Model (2)—8 ground supports

supports is increased, which results in an increase in the natural vibrations of the machine.

4.5.2 Static structural analysis—modified design

The machine is analyzed in static condition, and the parts are maintained in the resting position, similar to the analysis earlier. All of the conditions are identical, except for the fixed-support region. The boundary conditions, such as gravity and the amount of externally applied force, are one and the same. Model (2) was tested earlier, and the results are displayed in Fig. 17b. The total deformation of the system is 7.61 μm . Model (1), with a plain base, has a static deformation of 5.8 μm under same loading condition of 500 N external force on the tool turret. The obtained solution is displayed in Fig. 17.

The base is firmly fixed to the ground, avoiding any minor movement to a large extent. The total deformation demonstrates a great decline compared with the original model. As the machine rigidity increases with the increase in the surface area in contact with the ground, the final condition of having more supports to fix the base would be an appropriate possible design modification for future advancements. Model (3) has an increased number of ground fixtures, and

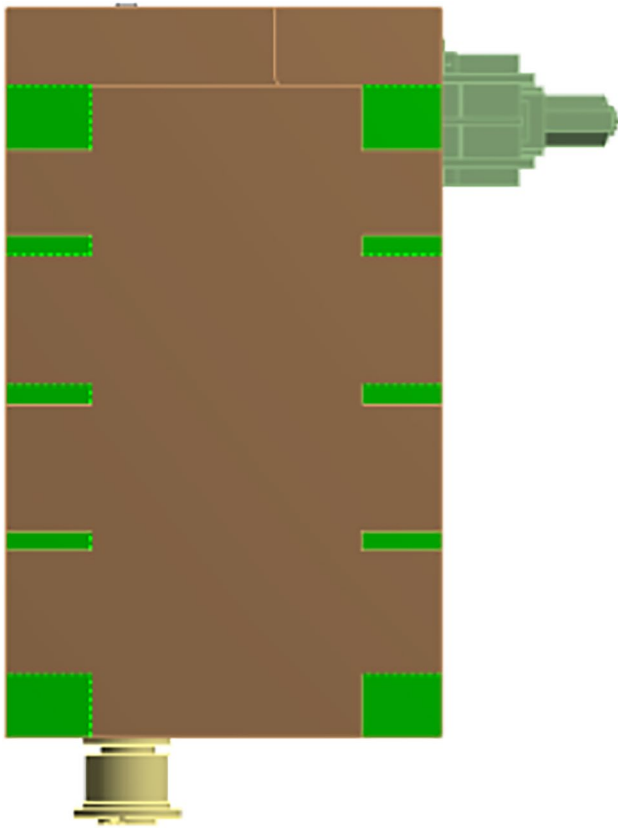


Fig. 15 Model (3)—10 ground supports

Table 7 Frequency table, model (1)

Mode	Frequency (Hz)
1	118.2
2	139.7
3	200.7
4	213.7
5	246.2
6	255.7
7	292.8
8	325.8
9	350.1
10	359.7

the static deformation is given in Fig. 15. The obtained result is anticipated by the preceding result. The machine has a total deformation of 6.8 μm , with a stable base compared with the original construction. The results are plotted together to provide comprehensive detail of the solutions, as shown in Fig. 18.

The displacement of the components decreases with an increase in the number of ground fixtures, allowing the machine to sustain greater loading conditions. Gao et al. [36]

Table 8 Frequency table, model (2)

Mode	Frequency (Hz)
1	108.2
2	133.4
3	191.7
4	207.1
5	210.9
6	223.1
7	2257.2
8	277.6
9	318.5
10	328.6

Table 9 Frequency table, model (3)

Mode	Frequency (Hz)
1	110.0
2	136.6
3	196.5
4	211.5
5	221.6
6	236.0
7	273.1
8	300.8
9	332.7
10	350.4

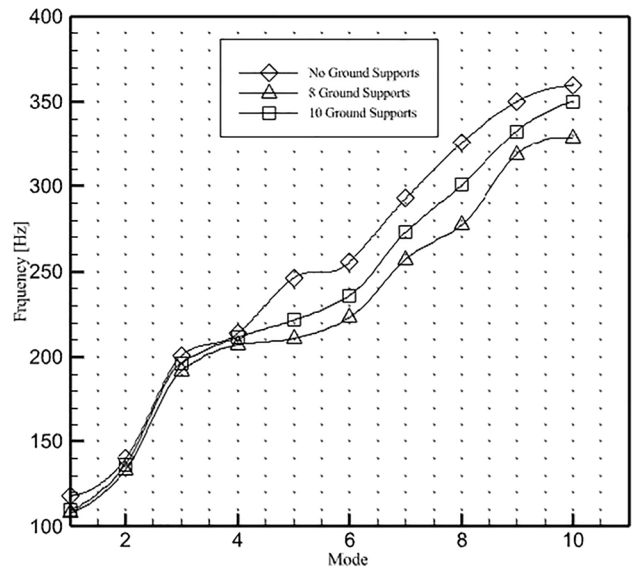


Fig. 16 Comparison study of the frequency versus mode data of the three different models

using the topology optimization module in ANSYS workbench, improved the static and dynamic performance of a work table by reducing its overall weight by 23.2 kg. This

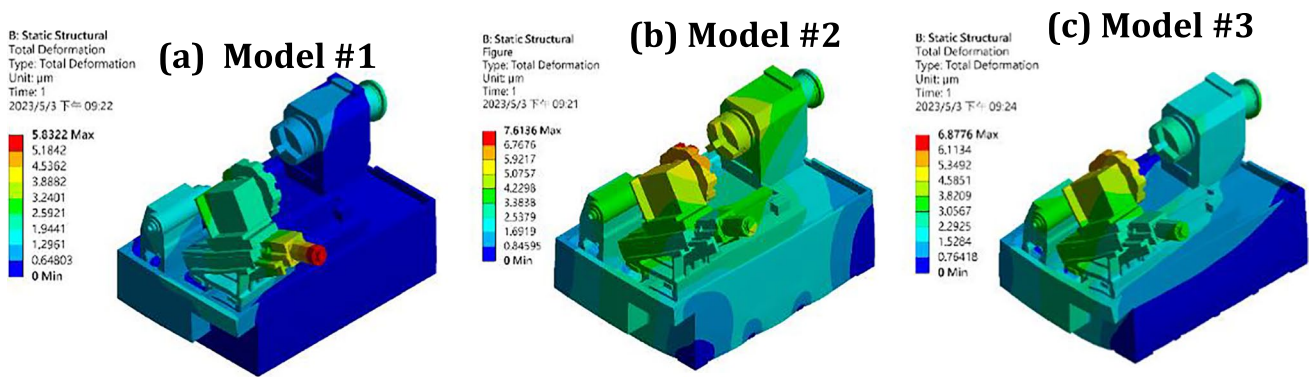


Fig. 17 Static structural analysis—modified design a model 1, b model 2, and c model 3

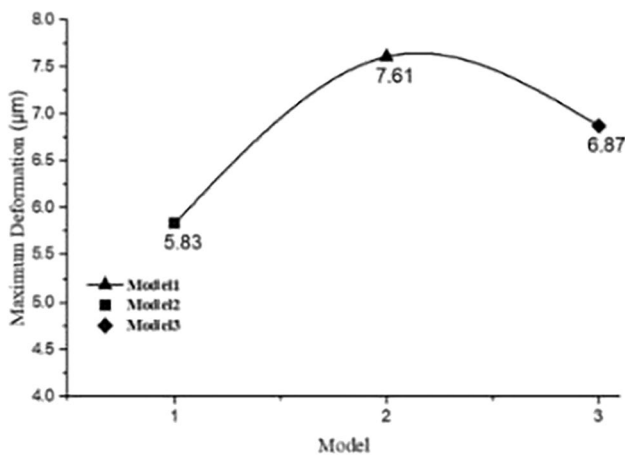


Fig. 18 Static deformation comparison, model (1, 2, 3)

research adapts the same module to optimize the bed of the machine in order to improve its dynamic performance.

4.6 Topology optimization

To show an overview of a methodology that incorporates analysis and optimization procedures based on nonlinear dynamic finite element analysis. Woytowicz et al. [37] studied that dynamic nonlinear finite element analysis can analyze and optimize structures undergoing huge motions. It is rigorous and computationally efficient. The methodology uses a broad objective function and constraint definition. Cheng et al. [38] used FEA to simulate SWG meshing and a two-step optimization technique to increase SWG performance. A Tcl script integrated a mathematical model, mesh creation program (Visual C++ codes), FEA solver, and optimization solver during optimization. According to simulations, optimization decreased the SWG's torsional angle by 9.76%, hysteresis loss by 17.63%, maximum stress on the FS's tooth surface by 22.24%, fatigue safety factor by 24.19%, and peak-to-peak gearbox error by 23.64%.

However, intriguing studies on structural optimization utilizing the Absolute Nodal Coordinates Formulation (ANCF) have been published [39–43]. In this study, an alternative way to increase the rigidity of the base is to utilize topology optimization analysis in the ANSYS workbench. The base of the machine is analyzed for modal frequencies and stress–strain contours. Topology optimization reduces the weight of the machine without affecting its design characteristics. The analysis is set to restrain 90% of the actual mass as a preliminary precaution to not change too much of the design analysis, which displays the area that is not influenced by any stress due to the weight of the parts lying on it. The marked area can be cleared using an engineering design; the modified design is reanalyzed, and the results are compared. This study's computer-aided design and optimization procedure can enhance the structure of industrial machines using the workflow of topology optimization shown in Fig. 19.

4.6.1 Pre-modification (machine bed)

Typically, the empirical procedure is utilized to design machine-tool castings. If not optimized, there may be an excess of materials. To attain high speed and accuracy, the structure is computer-optimized, resulting in significant material savings. Unnecessary material removal improves mechanical properties and reduces the cost of the machine tool. Using topology optimization, the structure of the machine tool was optimized in this investigation. The optimization objectives included maximization of rigidity, enhancement of natural frequency, and quality. Maximizing rigidity was the objective here. The model was then modified based on the optimized results, and both the original and optimized models were incorporated into the software for static analysis using finite element analysis. Comparative modal analyses were also conducted. Finally, a comparison was made between the results of the modified model and the entire machine analysis. In this study, a novel computational approach is developed for the gradient-based stress-based

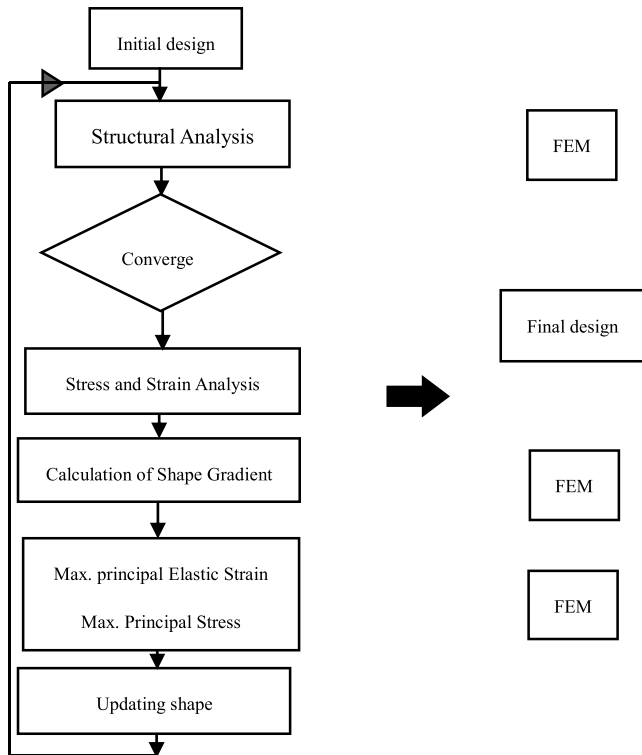


Fig. 19 Workflow of topology optimization

topology optimization method, in which the volume is minimized in accordance with locally defined stress constraints of static failure criteria within the framework of customized finite element (FE) software without direct access to an internal finite element information database. For stress-based topology optimization with solid isotropic material and penalized methods, tailored finite elements that require substantial understanding and modification and do not explicitly provide internal finite element information have been used infrequently. Modal analysis is applied to the machine bed to find the internal excitation of the bed alone. The weight of the part is 4987.7 kg, as given in the properties section of the ANSYS workbench. The obtained frequencies are displayed in Fig. 20. Static structural analysis is carried out to determine the stress and strain contours due to the weight of the parts lying on the bed. A representation

of the weight acting on the bed due to the parts lying on the slider rails is displayed in Fig. 21.

The analysis is set to restrain 90% of the mass, as mentioned earlier, and the optimization region is described as shown in Fig. 22. Torstenfelt et al. [44] proposed an effective pre-3D CAD tool for optimizing structural parameters of modules shared by-products in the same product family platform. This type of analysis will help determine the product’s most significant load-carrying structural components’ cross-sectional qualities in the first 3D CAD model.

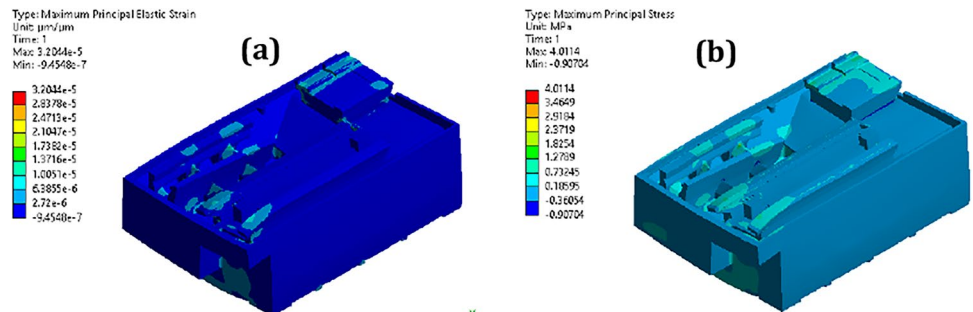
The important sections that, when altered, directly affect the dynamic characteristics of the machine are excluded from the analysis. For the above-mentioned boundary setting, the optimized results are shown in Fig. 23.

4.6.2 Post-modification

It has long been assumed that doing topology optimization while considering local stress limitations in the scope of customized finite element code with only basic post-processing information is difficult or impossible. To disprove this notion, we created a novel approach that uses only basic finite element post-processing data for stress-based topology optimization, decreasing the volume while considering local stress limitations. The machine bed is redesigned, and the weight of the body is reduced to 4940.6 kg, which is a mass reduction of 47.1 kg. The body is reanalyzed using modal and structural analysis and checked for improvements. The results are displayed in Figs. 24 and 25.

The contours remain unchanged after the modification, and the frequency range is increased, making the bed more rigid than in the earlier version. The design space, objectives, and variables (also known as the optimization parameters) are presented from a computational perspective. The machine was considered when using the compliance objective. The outcomes were improved by sub-modeling. Both center- and off-center-loaded situations were taken into consideration. New designs for the machine bed were created based on the findings. The comparison of the optimized and conventional designs shows that weight reduction and improvement are possible (depending on the machine’s production process).

Fig. 20 Stress and strain contours (pre-modification). a Max. principal elastic strain; b max. principal stress



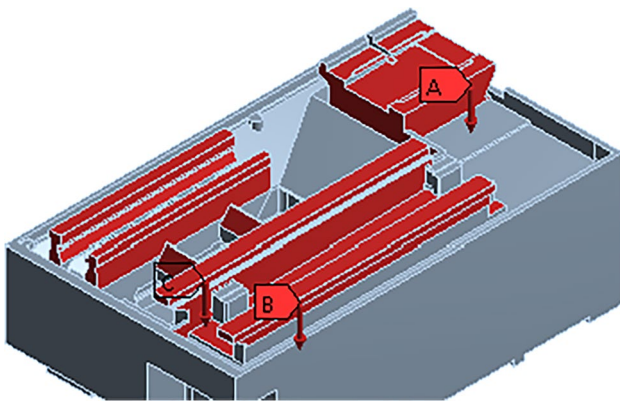


Fig. 21 Weight-induced areas on the base

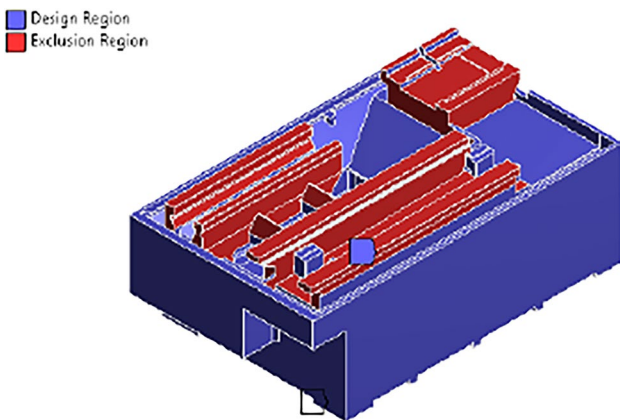


Fig. 22 Analysis region setting

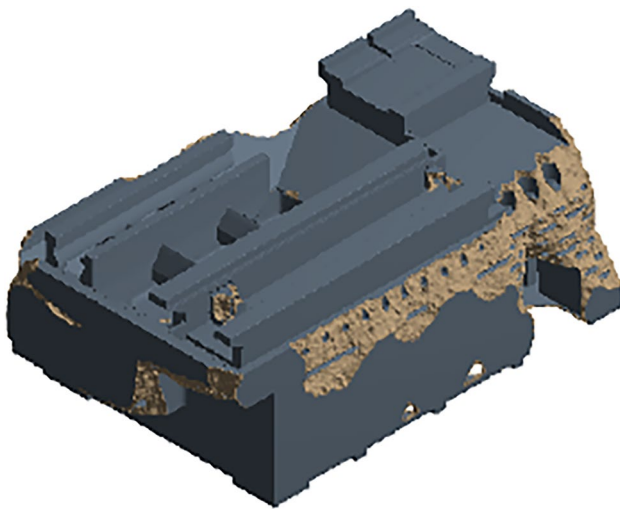


Fig. 23 Topology optimization result

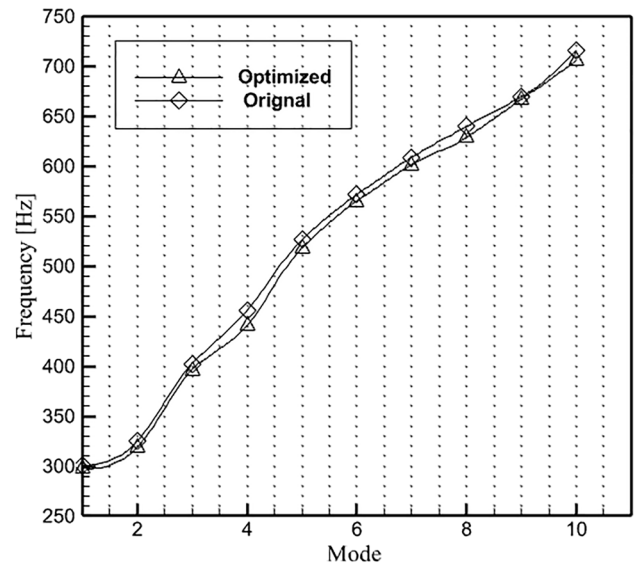


Fig. 24 Comparison between optimized bed and original internal frequency table

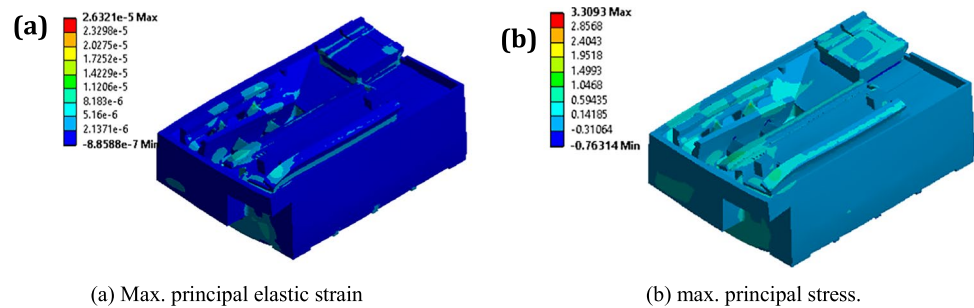
The new designs are easier to produce, more cost-effective, and environmentally friendly. Finally, this was done to improve the quality of the surfaces produced by the manufacturing procedures.

5 Conclusions

This study simplified a complex multi-body design into a feasible model to extract the static and dynamic characteristics. Although several other features of the ANSYS workbench software, such as damping, were not prioritized in this study, it can be an influential platform for engineers to design and analyze various mechanical engineering problems. The process of FEA started with modal analysis to evaluate the internal frequencies of the machine. The influence of the machine frequency in each mode implies a certain displacement of a part in the machine, affecting its machining process. The feasibility of impact hammer testing is adequate for engineering procedures.

The CAD model validated with an error in the sensible range allows us to continue with other analyses. The static, harmonic, and transient analyses evaluate the machine under various loading conditions, describing the machine’s performance. The dynamic and static analyses show the behavior of the machine under preloaded conditions resembling the working state. The closer the parts, the lesser the deformation, which is a beneficial factor while machining. The variation in the modal features varies linearly along with the movement of the parts, as displayed by the spatial analysis. When the

Fig. 25 Stress and strain contours (post-modification)



working conditions are filtered out, the amount of displacement varies with the positioning of the tool turret. The effect of gravity and the externally applied force on the machine tends to change with respect to the position of the parts. Redesigning the bed of the machine helps to improve its stability by a small margin, allowing it to meet the user's needs. Evenly spread ground supports have slightly higher-order internal vibrations compared with the original design. As the surface contact area increases, the machine's rigidity improves, providing a firm base. The model that is fully placed on the ground is more rigid than other models. This condition can be predicted, as the more ground contact, the more stable the body will be.

The modal analysis result increased by 2.16% on average for the first three modes. The static deformation exhibited a 10.2% decrease in the amount of total displacement in the moving components. The topology optimization of the base improved the internal frequencies of the base without affecting its original features. An increase in the vibration range reduces the likelihood of the machine experiencing resonance that could disturb the machining. The body weight of the CNC bed is reduced by 0.9% without drastically changing its shape, and the results improved by 1.03%, 1.9%, and 1.6% for the first three modes of the natural frequency. An average increase of 1.51% in the stability of the base improves the rigidity of the whole machine. A reduction of 45 kg in weight has a noticeable benefit for the structure without affecting its originality. The factors of rigidity, stiffness, and deformation are ideal for any operating mechanism. The extent of these features has a noticeable effect on the processing quality of the machine. Dynamic feature evaluation helps us learn about such machines. A lathe machine is used in surface finishing and in making assembly fixtures, which demands the best possible accuracy.

Acknowledgements The authors are indebted to the National Science and Technology Council (Grant numbers: 111-2221-E-150-024-MY2 and 111-2622-E-150-009).

Author contribution Experiment: S. Reddy. Analysis: Aman U and S. Reddy. Methodology: T.-C. Chan and S. Reddy. Validation: S. Reddy. Original draft preparation: Aman U, S. Reddy, and B. Roy. Supervision: T.-C. Chan.

Declarations

Competing interests The authors declare no competing interests.

References

- Kurowski PM (2022) Finite element analysis for design engineers. SAE International. <https://doi.org/10.4271/R-449>
- Doyle R, Case K (1990) CAE software in manufacturing engineering education. Computer Assisted Learning. Pergamon, pp 277–288. <https://doi.org/10.1016/B978-0-08-040249-9.50043-X>
- Zaeh M, Siedl D (2007) A new method for simulation of machining performance by integrating finite element and multi-body simulation for machine tools. CIRP Ann 56(1):383–386. <https://doi.org/10.1016/j.cirp.2007.05.089>
- Mackerle J (1999) Finite-element analysis and simulation of machining: a bibliography (1976–1996). J Mater Process Technol 86(1–3):17–44. [https://doi.org/10.1016/S0924-0136\(98\)00227-1](https://doi.org/10.1016/S0924-0136(98)00227-1)
- Zaghbani I, Songmene V (2009) Estimation of machine-tool dynamic parameters during machining operation through operational modal analysis. Int J Mach Tool Manuf 49(12–13):947–957. <https://doi.org/10.1016/j.ijmachtools.2009.06.010>
- Besharati SR et al (2016) Multi-objective selection and structural optimization of the gantry in a gantry machine tool for improving static, dynamic, and weight and cost performance. Concurr Eng 24(1):83–93. <https://doi.org/10.1177/1063293X15597047>
- Tunc LT, Mohammadi Y, Budak E (2018) Destabilizing effect of low frequency modes on process damped stability of multi-mode milling systems. Mech Syst Signal Process 111:423–441. <https://doi.org/10.1016/j.ymsp.2018.03.051>
- Chan TC, Lin HH, Reddy SV (2022) Prediction model of machining surface roughness for five-axis machine tool based on machine-tool structure performance. Int J Adv Manuf Technol 120(1–2):237–249. <https://doi.org/10.1007/s00170-021-08634-7>
- Chan TC et al (2022) Simulation, modeling, and experimental verification of moving column precision grinding machine. J Chin Inst Eng 45(1):54–64. <https://doi.org/10.1080/02533839.2021.1983464>
- Mbarek A et al (2018) Comparison of experimental and operational modal analysis on a back to back planetary gear. Mech Mach Theory 124:226–247. <https://doi.org/10.1016/j.mechmachtheory.2018.03.005>
- Yang B et al (2019) Kinematic modeling and machining precision analysis of multi-axis CNC machine tools based on screw theory. Mech Mach Theory 140:538–552. <https://doi.org/10.1016/j.mechmachtheory.2019.06.021>
- Wang M et al (2022) Dimensional parameters and structural topology integrated design method of a planar 5R parallel machining

- robot. *Mech Mach Theory* 175:104964. <https://doi.org/10.1016/j.mechmachtheory.2022.104964>
13. Chauhan S et al (2011) Operational modal analysis of operating wind turbines: application to measured data. *Rotating Machinery, Structural Health Monitoring, Shock and Vibration, Volume 5: Proceedings of the 29th IMAC, A Conference on Structural Dynamics*, 2011 pp (65–81). New York, NY: Springer New York. https://doi.org/10.1007/978-1-4419-9428-8_6
 14. Chen D, Fan J, Zhang F (2012) Dynamic and static characteristics of a hydrostatic spindle for machine tools. *J Manuf Syst* 31(1):26–33. <https://doi.org/10.1016/j.jmsy.2010.11.006>
 15. Wu Z et al (2010) Modal and harmonic response analysis and evaluation of machine tools. 2010 International Conference on Digital Manufacturing & Automation. Vol. 1, pp 929–933 IEEE. <https://doi.org/10.1109/ICDMA.2010.155>
 16. Lu X, Chen Y, Sheng X (2022) Analysis of the influence of structural parameters on the modes of a gantry machine tool crossbeam based on analytical method. *Appl Sci* 12(21):11083. <https://doi.org/10.3390/app122111083>
 17. Chan TC, Yang JS (2020) Optimized design and performance study of high speed five-axis machine tools. In: *International Design Engineering Technical Conferences and Computers and Information in Engineering Conference*, vol 83952. American Society of Mechanical Engineers. <https://doi.org/10.1115/DETC2020-22253>
 18. Hong CC, Chang CL, Lin CY (2016) Static structural analysis of great five-axis turning–milling complex CNC machine. *Eng Sci Technol* 19(4):1971–1984. <https://doi.org/10.1016/j.jestch.2016.07.013>
 19. Chan TC et al (2023) Study on kinematic structure performance and machining characteristics of 3-axis machining center. *Appl Sci* 13(8):4742. <https://doi.org/10.3390/app13084742>
 20. Huo D, Cheng J, Wardle F (2010) Design of a five-axis ultra-precision micro-milling machine—UltraMill. Part 1: holistic design approach, design considerations and specifications. *Int J Adv Manuf Technol* 47:867–877. <https://doi.org/10.1007/s00170-009-2129-1>
 21. Li X et al (2021) Structural design and optimization of the crossbeam of a computer numerical controlled milling-machine tool using sensitivity theory and NSGA-II algorithm. *Int J Precis Eng Manuf* 22:287–300. <https://doi.org/10.1007/s12541-020-00435-4>
 22. Deng C et al (2015) Dynamic characteristics optimization for a whole vertical machining center based on the configuration of joint stiffness. *Int J Adv Manuf Technol* 76:1225–1242. <https://doi.org/10.1007/s00170-014-6355-9>
 23. Qiu L et al (2022) Research on the line-arc-line constant-torque flexure hinge (LAL-CTFH) based on improved pseudo-rigid-body model (PRBM). *Mech Mach Theory* 174:104878. <https://doi.org/10.1016/j.mechmachtheory.2022.104878>
 24. Ji Q et al (2020) Structural design optimization of moving component in CNC machine tool for energy saving. *J Clean Prod* 246:118976. <https://doi.org/10.1016/j.jclepro.2019.118976>
 25. Zhong G et al (2018) Design optimization approach of a large-scale moving framework for a large 5-axis machining center. *Appl Sci* 8(9):1598. <https://doi.org/10.3390/app8091598>
 26. Park HW, Park YB, Steven Y, Liang (2011) Multi-procedure design optimization and analysis of mesoscale machine tools. *Int J Adv Manuf Technol* 56: 1–12. <https://doi.org/10.1007/s00170-011-3160-6>
 27. Wang KC, Yang CH (2023) Structural design optimization of movable-column horizontal machining center based on integral stiffness analysis and sensor measurement. *Sens Mater* 35:10.18494/SAM4117
 28. Ibrahim AM, Ali AM, Kamel H (2023) Design optimization and production of a small-scale semi-trailer chassis for testing. *J Eng Appl Sci* 70(1):35. <https://doi.org/10.1186/s44147-023-00201-z>
 29. Zienkiewicz OC, Morice PBFF (1971) *The finite element method in engineering science*, vol 1977. McGraw-hill, London <https://lccn.loc.gov/76028984>
 30. Bathe KJ, Wilson EL (1976) *Numerical methods in finite element analysis*. (No Title). <https://lccn.loc.gov/75046522>
 31. White DA et al (2023) A reduced order model approach for finite element analysis of cellular structures. *Finite Elem Anal Des* 214:103855. <https://doi.org/10.1016/j.finel.2022.103855>
 32. Gil J et al (2022) Finite element periodic catenary model to perform HIL pantograph tests considering non-linear dropper behaviour. *Finite Elem Anal Des* 210:103816. <https://doi.org/10.1016/j.finel.2022.103816>
 33. Tlustý J, Ismail F (1983) Special aspects of chatter in milling:24–32. <https://doi.org/10.1115/1.3269061>
 34. Bais RS et al (2004) Studies in dynamic design of drilling machine using updated finite element models. *Mech Mach Theory* 39(12):1307–1320. <https://doi.org/10.1016/j.mechmachtheory.2004.05.022>
 35. Schwarz BJ, Richardson MH (1999) Experimental modal analysis. *CSI Reliability Week* 35(1):1–12
 36. Gao DQ et al (2011) Finite element analysis and structure optimization of machine tool worktable. *Appl Mech Mater* 80:985–989. <https://doi.org/10.4028/www.scientific.net/AMM.80-81.985>
 37. Woytowicz PJ, Hight TK (1994) Optimization of controlled flexible mechanisms using dynamic nonlinear finite element analysis. *Mech Mach Theory* 29(7):941–958. [https://doi.org/10.1016/0094-114X\(94\)90063-9](https://doi.org/10.1016/0094-114X(94)90063-9)
 38. Cheng YH, Chen YC (2022) Design, analysis, and optimization of a strain wave gear with a novel tooth profile. *Mech Mach Theory* 175:104953. <https://doi.org/10.1016/j.mechmachtheory.2022.104953>
 39. Yakoub RY, Shabana AA (2001) Three dimensional absolute nodal coordinate formulation for beam elements: implementation and applications. *J Mech Des* 123(4):614–621. <https://doi.org/10.1115/1.1410099>
 40. Shabana A, Yakoub RY (2001) Three dimensional absolute nodal coordinate formulation for beam elements: theory. *J Mech Des* 123(4):606–613. <https://doi.org/10.1115/1.1410100>
 41. Tian Q et al (2009) An efficient hybrid method for multibody dynamics simulation based on absolute nodal coordinate formulation:021009. <https://doi.org/10.1115/1.3079783>
 42. Gerstmayr J, Irschik H (2008) On the correct representation of bending and axial deformation in the absolute nodal coordinate formulation with an elastic line approach. *J Sound Vib* 318(3):461–487. <https://doi.org/10.1016/j.jsv.2008.04.019>
 43. García-Vallejo D et al (2004) Efficient evaluation of the elastic forces and the Jacobian in the absolute nodal coordinate formulation. *Nonlinear Dyn* 35:313–329. <https://doi.org/10.1023/B:NODY.0000027747.41604.20>
 44. Torstenfelt B, Klarbring A (2007) Conceptual optimal design of modular car product families using simultaneous size, shape, and topology optimization. *Finite Elem Anal Des* 43(14):1050–1061. <https://doi.org/10.1016/j.finel.2007.06.005>

Publisher's note Springer Nature remains neutral with regard to jurisdictional claims in published maps and institutional affiliations.

Springer Nature or its licensor (e.g. a society or other partner) holds exclusive rights to this article under a publishing agreement with the author(s) or other rightsholder(s); author self-archiving of the accepted manuscript version of this article is solely governed by the terms of such publishing agreement and applicable law.